

See discussions, stats, and author profiles for this publication at: <https://www.researchgate.net/publication/231271205>

# Crystallization of Mixed Paraffin from Model Waxy Oils and the Influence of Micro-crystalline Poly(ethylene-butene) Random Copolymers

ARTICLE *in* ENERGY & FUELS · JUNE 2004

Impact Factor: 2.79 · DOI: 10.1021/ef034098p

CITATIONS

31

READS

57

6 AUTHORS, INCLUDING:



**Brian A Pethica**

Princeton University

172 PUBLICATIONS 3,834 CITATIONS

SEE PROFILE



**Robert K Prud'homme**

Princeton University

283 PUBLICATIONS 12,866 CITATIONS

SEE PROFILE



**Douglas H. Adamson**

University of Connecticut

114 PUBLICATIONS 8,744 CITATIONS

SEE PROFILE

# Crystallization of Mixed Paraffin from Model Waxy Oils and the Influence of Micro-crystalline Poly(ethylene-butene) Random Copolymers

Xuhong Guo,<sup>†</sup> Brian A. Pethica,<sup>†</sup> John S. Huang,<sup>†</sup> Robert K. Prud'homme,<sup>\*,†</sup> Douglas H. Adamson,<sup>‡</sup> and Lewis J. Fetters<sup>§</sup>

Department of Chemical Engineering, Princeton University, Princeton, New Jersey 08544, Princeton Materials Institute, Princeton University, Princeton, New Jersey 08544, and School of Chemical and Biomolecular Engineering, Cornell University, Ithaca, New York 14853-5210

Received December 5, 2003

We report rheological, microscopic, and calorimetric studies of the crystallization of long chain *n*-paraffins and their mixtures from model waxy oils and the effect of microcrystalline poly(ethylene-butene) (PEB) random copolymers. Optical micrographs and differential scanning calorimetry (DSC) reveal that the crystals formed from decane solutions of binary mixtures of C36 + C32 and of C32 + C28 are of mixed composition, whereas solutions of C28 + C24, C36 + C28, C32 + C24, and C36 + C24 form separate crystal phases. There is no miscibility when the difference in carbon number between two long chain *n*-paraffins  $\Delta n_c > 4$ . These findings agree with Kravchenko's prediction for crystallization of molten binary *n*-alkane mixtures. However, the crystallization of long chain *n*-paraffins from decane solution gives a stable crystal structure directly, while from the melt it tends to pass through a metastable rotator phase. Since PEB can either self-assemble into a needlelike structure or cocrystallize with long chain *n*-paraffins to form small thin sheets in decane, mixtures of wax and PEB formed quite complex shapes such as rodlike or shuttle-like structures, particularly for the longer paraffin chains. These structures reduce the yield stress of the cold model waxy oil as compared with the platelike crystals formed in the absence of PEB. PEB10, which has an average of 10 ethyl side groups per 100 carbon atoms in the polymer backbone, is more effective in reducing the yield stress than PEB7.5 except for the mixture C36 + C28. All the other mixtures of paraffins with PEBs show intermediate rheological properties between those of the single paraffin components.

## Introduction

Wax deposition on the wall of cold pipelines is a persistent problem in the oil industry. Deposition restricts flow and can lead to plugging of the pipelines. It becomes more significant when the production wells are located offshore because deep ocean water is typically at 4 °C.<sup>1,2</sup> Polymer additives, such as ethyl-vinyl acetate copolymer (EVA),<sup>3</sup> polyethylene-poly(ethylene-propylene) (PE-PEP)<sup>4–7</sup> and poly(ethylene-butene)

(PEB)<sup>8,9</sup> are able to improve the rheological properties of waxy oil by modifying the wax crystal structures, and thus reducing the deposition of wax on the pipe wall. Polymer treatments to prevent deposition and gelation can be more economical than mechanical (pigging) or thermal (heating) methods.<sup>10</sup>

Among the polymer modifiers, EVA and PE-PEP have received intensive investigation. PEB, a new candidate wax modifier, is a polymer with alternate crystalline and amorphous segments (Figure 1). It was found to be very effective in reducing the yield stress of model waxy oils.<sup>9</sup> Since the mechanism for flow improvement of these model waxy oils is still unclear, PEB was chosen as the wax crystal modifier in this work.

The crystallization, crystallographic structure, and the phase transition of pure and mixed *n*-alkanes<sup>11–13</sup> from melts<sup>14–20</sup> have been investigated intensively [see the review ref 21]. Few investigations have been made

\* Author to whom correspondence should be addressed. E-mail: prudhomme@princeton.edu.

<sup>†</sup> Department of Chemical Engineering, Princeton University.

<sup>‡</sup> Princeton Materials Institute, Princeton University.

<sup>§</sup> Cornell University.

(1) Singh, P.; Venkatesan, R.; Fogler, H. S.; Nagarajan, N. R. *AIChE J.* **2001**, *47*, 6–18.

(2) Ribeiro, F. S.; Souza, P. R.; Mendes, S.; Braga, S. L. *Int. J. Heat Mass Transfer* **1997**, *40*, 4319–4328.

(3) Gilby, G. W. *Special Publication—Royal Society of Chemistry, Chemicals in Oil Industry* **1983**, *45*, 108–124.

(4) Ashbaugh, H. S.; Fetters, L. J.; Adamson, D. H.; Prud'homme, R. K. *J. Rheol.* **2002**, *46*, 763–776.

(5) Schwahn, D.; Richter, D.; Wright, P. J.; Symon, C.; Fetters, L. J.; Lin, M. *Macromolecules* **2002**, *35*, 861–870.

(6) Leube, W.; Monkenbusch, M.; Schneiders, D.; Richter, D.; Adamson, D.; Fetters, L. J.; Dounis, P.; Lovegrove, R. *Energy Fuels* **2000**, *14*, 419–430.

(7) Richter, D.; Schneiders, D.; Monkenbusch, M.; Willner, L.; Fetters, L. J.; Huang, J. S.; Lin, M.; Moretenson, K.; Farago, B. *Macromolecules* **1997**, *30*, 1053–1068.

(8) Schwahn, D.; Richter, D.; Lin, M.; Fetters, L. J. *Macromolecules* **2002**, *35*, 3762–3768.

(9) Ashbaugh, H. S.; Radulescu, A.; Prud'homme, R. K.; Schwahn, D.; Richter, D.; Fetters, L. J. *Macromolecules* **2002**, *35*, 7044–7053.

(10) Denis, J.; Durand, J. P. *Rev. Inst. Fr. Pet.* **1991**, *46*, 637–649.

(11) Sirota, E. B.; Herhold, A. B. *Science* **1999**, *283*, 529–532.

(12) Sirota, E. B.; Singer, D. M. *J. Chem. Phys.* **1994**, *101*, 10873–10882.

(13) Crag, S. R.; Hastie, G. P.; Roberts, K. J.; Sherwood, J. N.; Tack, R. D.; Cernik, R. J. *J. Mater. Chem.* **1999**, *9*, 2385–2392.

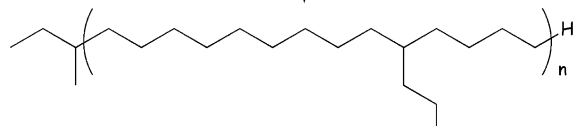


**Figure 1.** Chemical structure of poly(ethylene-butene) (PEB).

on the crystallization process and the crystal morphology of paraffin wax formed from solution.<sup>22</sup> We accordingly compare the crystallization of long chain paraffins from melts and decane solutions.

There are several reports on the effect of wax modifiers on single paraffins from melts and solutions<sup>4,8–9,23–25</sup> as well as studies on waxy crude oil compositions,<sup>1,3</sup> but studies of the modification of crystallization of paraffin mixtures are rather scarce. Thus, the study of the effect of wax modifiers on paraffin mixtures should help in understanding the relationship between polymer structure, wax carbon number, and the mechanism of wax gel modification.

In this paper, we address two questions: (1) what is the effect of paraffin mixtures on the yield stress of cooled model waxy oils, and (2) how different is the action of PEB on crystallization of single paraffins compared to paraffin mixtures from solution? Since the major components of wax separating from crude oil are linear paraffins,<sup>1</sup> we chose four linear paraffins with the number of carbon atoms of 24, 28, 32, and 36 as model paraffins and their solutions in decane as model waxy oils. This allows us to connect this study with our previous neutron scattering and rheology studies of pure component paraffin systems.<sup>4–9</sup>

## Experimental Section

**Materials.** Poly(ethylene-butene) (PEB) with a molecular weight of ca. 7000 g/mol and molecular weight distribution of 1.03 were prepared by Fetters and co-workers.<sup>26</sup> PEB was prepared by hydrogenation of the polydiene intermediate which was obtained by the anionic polymerization of 1,3-butadiene in mixed solvent of hexane and triethylamine with *tert*-butyllithium as the initiator. The ratio of 1,4-addition to 1,2-addition of butadiene was controlled by varying the proportion of hexane to triethylamine. Based on our previous study of single waxes, two polymers PEB7.5 and PEB10 were used in these experiments where the number denotes the ethyl side branches per 100 backbone carbons as determined via <sup>1</sup>H NMR.

Model waxy oil samples were prepared by dissolving long chain *n*-paraffin waxes in decane. Decane (anhydrous, 99+%, mp –30 °C), tetracosane (C24, 99%, F.W. 338.66, mp 49–52 °C), octacosane (C28, 99%, F.W. 394.77, mp 59 °C), dotriacon-

tane (C32, 97%, F.W. 450.88, mp 69 °C) and hexatriacontane (C36, 98%, F.W. 506.99, mp 74–76 °C) were purchased from Aldrich and used as obtained.

**Yield Stress Measurement.** The yield stress ( $\tau_y$ ) is defined as the stress below which no flow occurs. An operational definition of  $\tau_y$  was adopted as the stress at the transition between the creep and liquid-like viscosity regimes where  $\tau_y$  can be identified as the stress for which the derivative is a maximum.<sup>4</sup>

The yield stress measurements were performed on a Rheometrics DSR controlled stress rheometer with parallel plate geometry. The temperature was controlled to within 0.1 °C by a Peltier plate. The samples were initially heated to 70 °C to melt all wax and PEB crystals. To minimize evaporation, the sample was covered with a solvent trap and the temperature was rapidly decreased from 70 °C, the experimental test temperature, at the same cooling rate (ca. 30 °C/min) for all samples. After allowing the sample to anneal at constant temperature under no stress for 20 min, a static stress was applied and incrementally increased every 10 s (100 stress increments per decade) and the viscosity measured. The initial applied stress was chosen well below the stress at which creep begins.

**Optical Microscopy.** Wax crystal morphologies were observed using a Nikon TE200 inverted microscope with phase and DIC optics (Micron Optics, Cedar Knoll, NJ). Images were captured using a Kodak ES 310 CCD camera connected to a PC via a PIXCID imaging board (EPIX, Buffalo Grove, IL). Samples were initially heated to 70 °C and then quenched to 0 °C in ca. 2 min. Stored in ice until the measurement, a small amount of wax crystal was loaded onto the glass slide inside a copper stage with a central window. During the measurement, the temperature of the copper stage was controlled at 0 °C by a circulating bath.

**Differential Scanning Calorimetry (DSC).** The Perkin-Elmer Pyris 1 DSC thermal analyzer system was used for the differential scanning calorimetry (DSC) measurements. The temperature scale of the instrument was calibrated by the melting temperature of ice from DI water and the heat flow by the fusion of an indium standard. An empty steel sample pan was used as the reference. The DSC scans for the paraffins and model waxy oils were measured by weighting approximately 20 mg of the sample into a hermetically sealed stainless steel pan, and then placing the pan into the DSC sample tray. The samples were cooled at a rate of 10, 5, or 1 °C/min, from 70 °C to –25 °C unless otherwise stated and then heated back to 70 °C at the same rate. The heating and cooling experiments were done with the cells under a dry nitrogen atmosphere. The enthalpies of crystallization and melting for model wax were calculated from the area of peaks using the Pyris software.

**Wide Angle X-ray Scattering (WAXS).** Two-dimensional WAXS images were collected from powder samples of C36 crystals from both decane solution and from the melt in the transmission geometry using an evacuated Statton camera manufactured by W. H. Warhus. X-rays with a source wavelength of 0.154 nm were produced using a sealed tube generator with a Cu target and a Huber graphite monochromator. The WAXS patterns were recorded using Kodak image plates with the storage phosphors being read by a Molecular Dynamics SI phosphorimager.

## Results and Discussion

**1. Mixtures of Paraffin Waxes without PEB.** Four linear paraffins C36, C32, C28, C24 and their binary mixtures were dissolved in decane to a weight concentration of 2% or 4%. The measured yield stresses are shown in Figure 2, where each point represents a separate sample cooled to the final temperature *T*.

- (14) Rademeyer, M.; Dorset, D. L. *J. Phys. Chem. B* **2001**, *105*, 5139–5143.
- (15) Crag, S. R.; Hastie, G. P.; Roberts, K. J.; Gerson, A. R.; Sherwood, J. N.; Tack, R. D. *J. Mater. Chem.* **1998**, *8*, 859–869.
- (16) Dorset, D. L. *Acta Cryst.* **1995**, *B51*, 1021–1028.
- (17) Gilbert, E. P. *Phys. Chem. Chem. Phys.* **1999**, *1*, 1517–1529.
- (18) Sirota, E. B.; King, H. E.; Shao, H. H.; Singer, D. M. *J. Phys. Chem.* **1995**, *99*, 798–804.
- (19) Sirota, E. B. *Phys. Rev. E* **2001**, *64*, 507011-4.
- (20) Giorgio, S.; Kern, R. *J. Cryst. Growth* **1983**, *62*, 360–374.
- (21) Dirand, M.; Bouroukba, M.; Chevallier, V.; Petitjean, D.; Behar, E.; Ruffier-Meray, V. *J. Chem. Eng. Data* **2002**, *47*, 115–143.
- (22) Abdallah, D. J.; Weiss, R. G. *Langmuir* **2000**, *16*, 352–355.
- (23) Holder, G. A.; Winkler, D. J. *Nature* **1965**, *207*, 719–721.
- (24) Beiny, D. H. M.; Mullin, J. W.; Lewtas, K. *J. Cryst. Growth* **1990**, *102*, 801–806.
- (25) Kern, R.; Dassonville, R. *J. Cryst. Growth* **1992**, *116*, 191–203.
- (26) Morton, M.; Fetters, L. *J. Rubber Chem. Technol.* **1975**, *48*, 358–409.

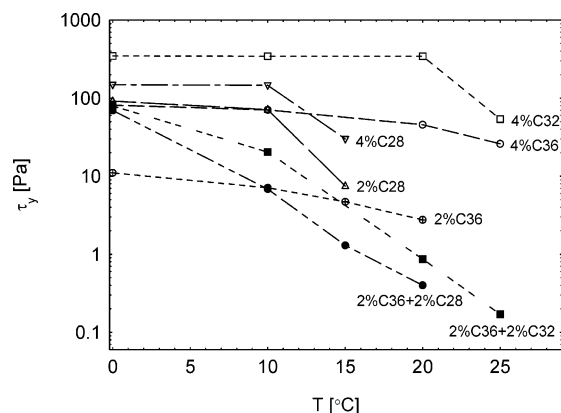


**Figure 2.** Yield stresses of paraffins and their mixtures in decane as a function of temperature. (○) 4% C36; (□) 4% C32; (▽) 4% C28; (△) 2% C28; (⊗) 2% C36; (■) 2% C36 + 2% C32; (●) 2% C36 + 2% C28.

It is interesting that the yield stresses of mixed paraffin solutions are much lower than those of each component. For example, the yield stress for 2%C36 + 2%C28 at 10 °C is 10 Pa, whereas the yield stresses for 4%C36 and 4%C28 are 80 and 120 Pa, respectively. In addition, the mixture of 2%C36 + 2%C32 shows higher yield stress than 2%C36 + 2%C28. For all mixtures (2% + 2%), the yield stress is lower than that for 4% of either component; the mix of paraffins decreases in yield (mixed paraffins have decreased yield) stresses.

In Figure 3, all the pure paraffins appear as large crystals, either as three-dimensional "house of cards"<sup>9</sup> for C36 and C32 or as long bars for C28 and C24. However, the binary mixtures show separated crystal lamellae with a size of ca. 50 μm. Indeed, mixed paraffins leads to different morphologies as compared with their pure components. Both the decreased size and separated lamellae will contribute to the diminution of yield stress.

In our previous study we have presented the solubility curves for C24, C28, C32, and C36 in decane as a function of temperature.<sup>4</sup> To address the relationship between the composition of the wax crystals, temperature, and rheology of wax mixtures, DSC was used to

monitor the crystallization behavior of paraffins and their mixtures in decane.

Surprisingly, as displayed in Figure 4a, C36 and C32 appear to cocrystallize at all ratios since only one exothermic crystallization peak can be observed over the entire composition range. The onset temperature changes from 35 °C (C36) to 28 °C (C32). However, the mixtures of C36 and C28 show two separated peaks in Figure 4b, indicating separate crystallization processes. Note that the lower temperature peak occurs at a lower temperature than the peak for pure C28. This reflects the lower crystallization temperature of more dilute wax compositions as would be predicted from the pure component solubility curve.<sup>4</sup> Further investigation on the binary mixtures using DSC shows that C32 and C28 also form mixed solids (Figure 5a), whereas C28 and C24 as well as C32 and C24 separate on cooling (Figure 5b).

To summarize, binary paraffin solutions in decane with a difference in the number of carbon atoms  $\Delta n_c \leq 4$  (C36 + C32 and C32 + C28) formed mixed solids. The other combinations, either  $n_c < 28$  (C28 + C24) or  $\Delta n_c > 4$  (C36 + C28, C32 + C24), crystallize separately upon cooling. Our observation agrees with Kravchenko's prediction for melts<sup>21,27</sup> that there is partial miscibility in the solid state for binary *n*-alkane mixtures with  $\Delta n_c = 4$  when  $68 > n_c > 27$  but no miscibility when  $n_c < 28$  for both long chain paraffins.

Now we can understand why 2%C36 + 2%C32 shows a higher yield stress than 2%C36 + 2%C28 (Figure 2). The miscibility between C36 and C32 allows cocrystallization and the formation of large crystals, which creates space-filling networks, while C36 and C28 crystallize separately and form many weak points between two kinds of lamellae.

The crystallization of C28 from melt and from decane solution is observed by DSC (Figure 6). It is interesting to see two peaks for pure C28 from melt, while only one for C28 from decane solution. Sirota and co-workers<sup>11,19</sup> have shown that the first (from the right) peak for pure C28 cooling from melt denotes crystallization to form a disordered rotator phase, and the second sharp peak shows a solid–solid phase transition from disordered

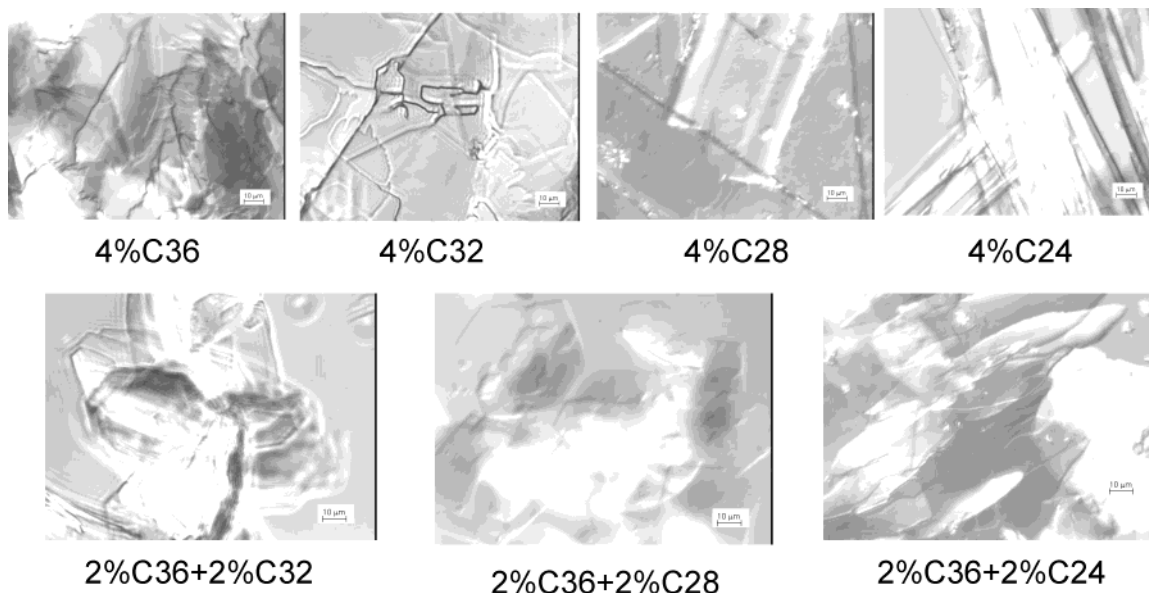


**Figure 3.** Optical micrographs of model wax crystals from decane at 0 °C.



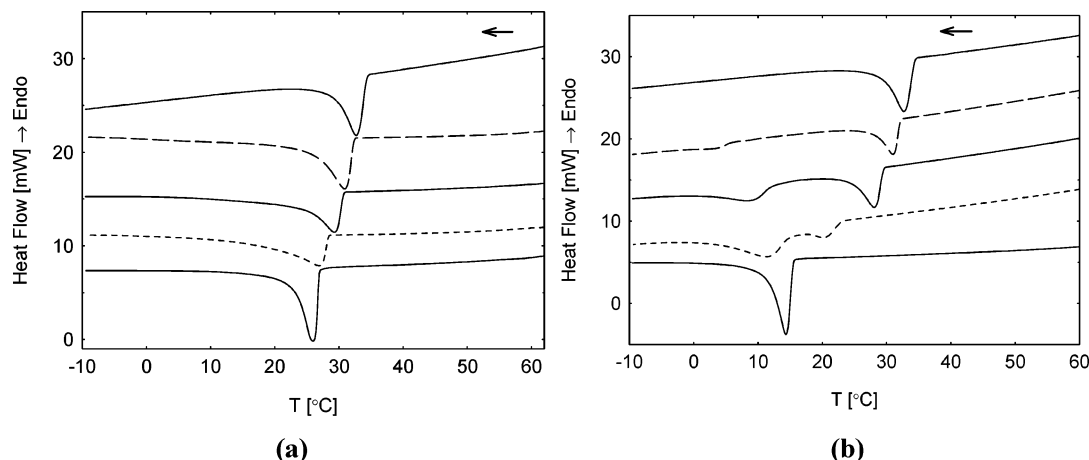


**Figure 4.** Differential scanning calorimetry (DSC) traces for paraffins and their mixtures in decane. (a) C36, C32, and their mixtures, curves from top to bottom denote 4%C36, 3%C36 + 1%C32, 2%C36 + 2%C32, 1%C36 + 3%C32, and 4%C32, respectively.; (b) C36, C28, and their mixtures, from top to bottom are 4%C36, 3%C36 + 1%C28, 2%C36 + 2%C28, 1%C36 + 3%C28, and 4%C28, respectively. The samples were cooled from 70 °C to −10 °C at the scanning rate of 10 °C/min.

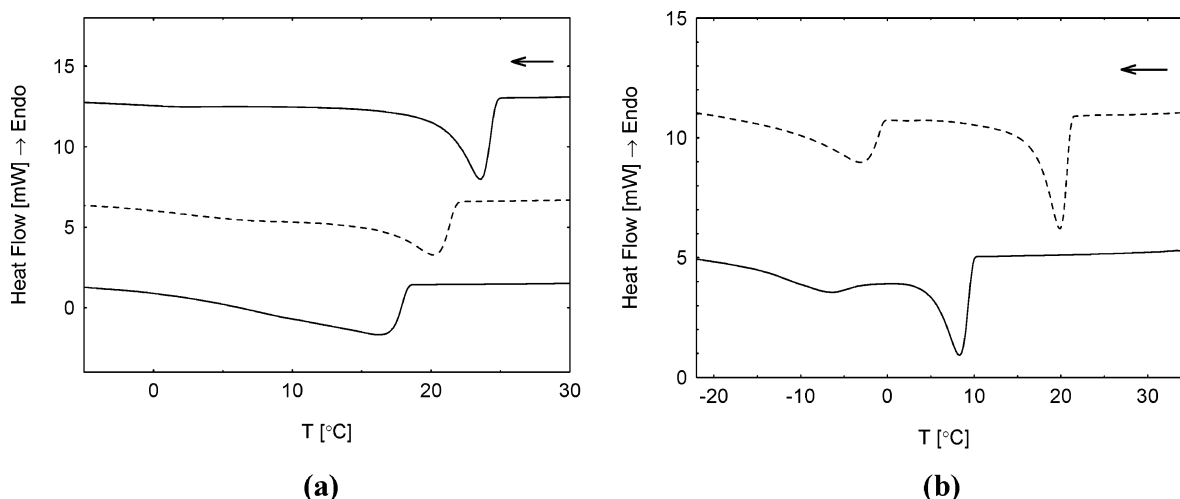


**Figure 5.** DSC curves of binary mixed paraffins in decane. (a) C32 + C28, from top to bottom denote to 3%C32 + 1%C28, 2%C32 + 2%C28, and 1%C32 + 3%C28, respectively. The samples were cooled from 70 °C to −10 °C at 10 °C/min; (b) 2%C32 + 2%C24 (dotted line) and 2%C28 + 2%C24 (solid line). The samples were cooled from 70 °C to −25 °C at 10 °C/min.

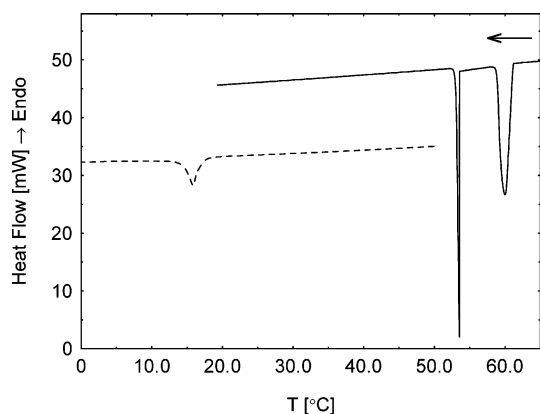


**Figure 6.** Comparison of DSC curves for different C28 samples. Curves from top to bottom are pure C28 (scan rate: 1 °C/min) and 4%C28 in decane (scan rate: 5 °C/min).

rotator phase to an ordered monoclinic structure. But no solid–solid transition peak can be detected for the crystallization of 4%C28 from decane.

The miscibility between C36 and C32 is also reflected in the DSC curves (Figure 7). The pure mixture of 50 wt % C36 + 50 wt % C32 shows two peaks such as the

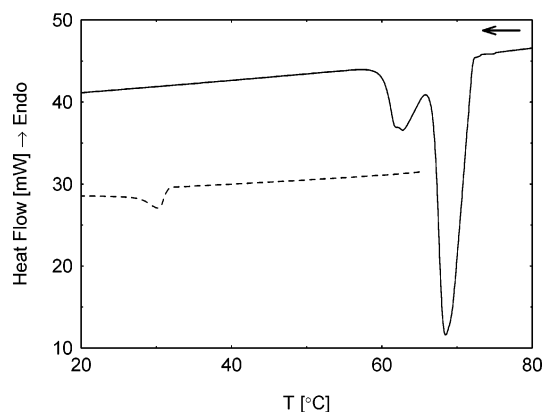


**Figure 7.** Comparison of DSC curves crystallization upon cooling of C36 + C32 mixtures. Solid curve is 50%C36 + 50%C32 solid mixture, while dotted line represents 2%C36 + 2%C32 in decane (scan rate: 5 °C/min from 80 to 10 °C).

single paraffin C28. The peak at higher temperature reflects the crystallization to form rotator phase and the other one represents the solid–solid phase transition (from rotator to monoclinic structure). The sample from decane solution shows only one peak (Figure 7).

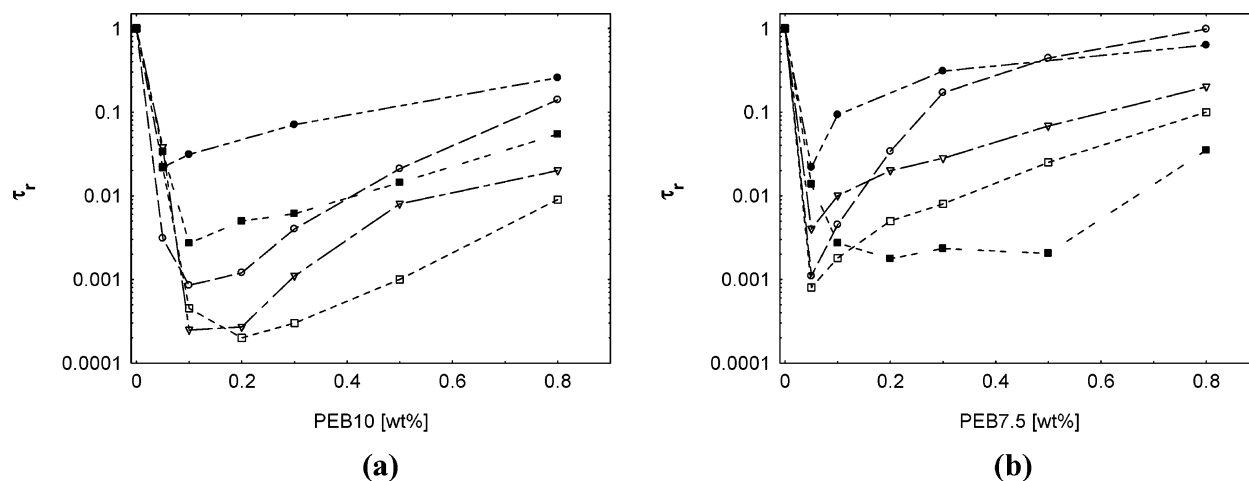


**Figure 8.** Effect of PEB7.5 (a) and PEB10 (b) on yield stress of paraffins and their mixtures in decane at 0 °C. (○) 4% C36; (□) 4% C32; (▽) 4% C28; (●) 2% C36 + 2% C32; (■) 2% C36 + 2% C28.

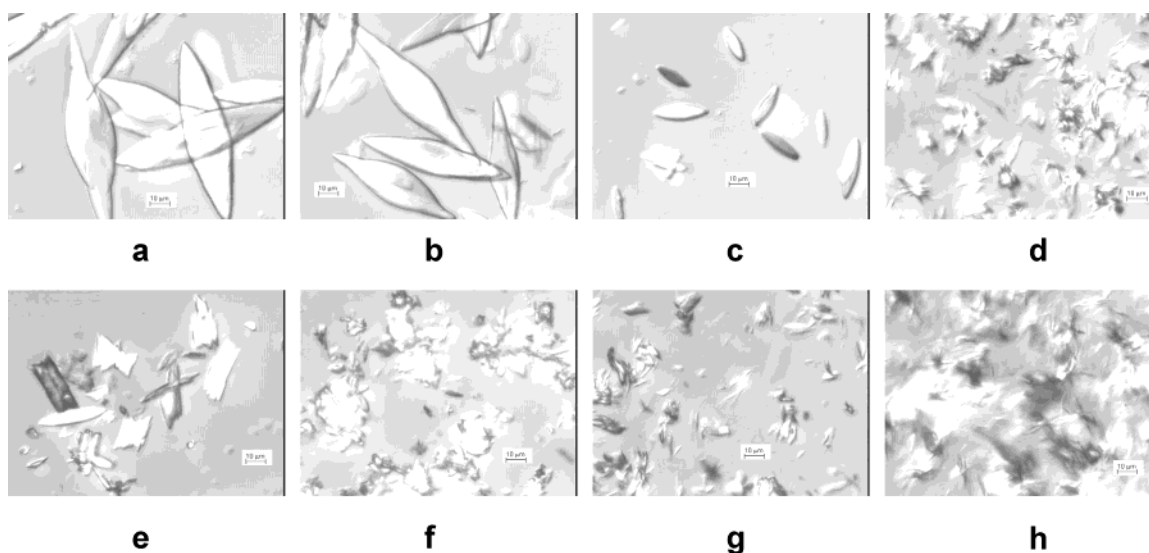


**Figure 9.** Optical micrographs of 4% C36 wax crystals under the effect of various amounts of PEB7.5 or PEB10 in decane at 0 °C. (a) 0.05 wt % PEB10; (b) 0.1 wt % PEB10; (c) 0.3 wt % PEB10; (d) 0.8 wt % PEB10; (e) 0.05 wt % PEB7.5; (f) 0.1 wt % PEB7.5; (g) 0.3 wt % PEB7.5; (h) 0.8 wt % PEB7.5.

**2. PEB Effect on Single Paraffins.** The addition of a small amount of PEB7.5 or PEB10 reduces the yield stresses of solutions of single paraffin and their mixtures significantly (Figure 8). Here we use the normalized yield stress (relative yield stress  $\tau_r$ ), which is defined as the ratio of the PEB-modified yield stress to the original yield stress without PEB, to describe the efficiency of PEB modification.

The microscopic crystal morphologies of C36 modified by PEB7.5 and PEB10 are compared in Figure 9. With the addition of PEB10, the crystals of C36 show shuttle-like structures, the size decreasing with increasing amounts of PEB10. In the case of PEB7.5, the shape of the crystals is irregular, but their size decreases with PEB7.5 addition. At the highest concentration (0.8 wt % PEB), both morphologies modified by PEB7.5 and PEB10 are similar: a gel consisting of numerous rodlike crystals.

Both PEB10 and PEB7.5 are semicrystalline random copolymers with ethylene and butylenes units.<sup>4,9</sup> The difference between them is the amount of ethyl side chains. PEB10 has an average of 10 ethyl side chains in a length of every 100 carbon atoms and thus is less

crystallizable than PEB7.5. From SANS observations,<sup>8,9</sup> PEB can either self-assemble into a needlelike structure (when PEB precipitates before the paraffin) or cocrystallize with the long chain paraffin to form a 2D planar structure (when paraffin cocrystallizes with PEB during cooling) in decane solution.<sup>9</sup> The formation of crystals with different shape and size as the ratio of polymer to wax varies is correlated to the macroscopic crystal habit (Figure 9). However, the mechanism whereby the crystals grow to form a shuttle shape in case of PEB10 and have a more irregular form with PEB7.5 is still not clear.

Although the crystal size of C36 modified by PEB7.5 is smaller than crystals modified by PEB10, the yield stresses are higher except with the sample with 0.05 wt % PEB7.5. It seems that the shuttle-like shape is favorable for reducing the yield stress.

Further insight on the effect of PEB on C36 crystallization is obtained by DSC (Figure 10). Two peaks appear for pure C36 from melt while only one appears for C36 from decane solution, even using the scan rate

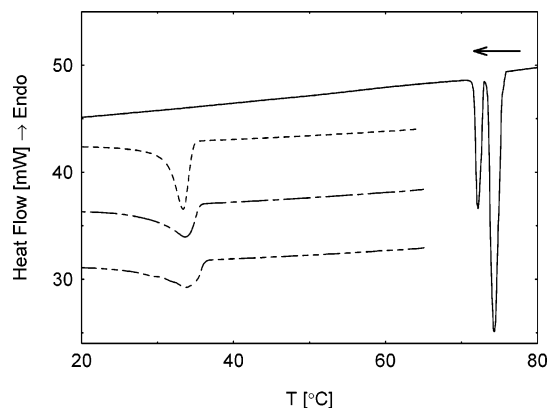


**Figure 10.** Comparison of DSC curves for different C36 samples. Curves from top to bottom are pure C36 (scan rate: 1 °C/min), 4%C36 in decane (scan rate: 5 °C/min), 4%C36 + 0.1%PEB7.5 (scan rate: 5 °C/min), and 4%C36 + 0.1%PEB10 (scan rate: 5 °C/min).

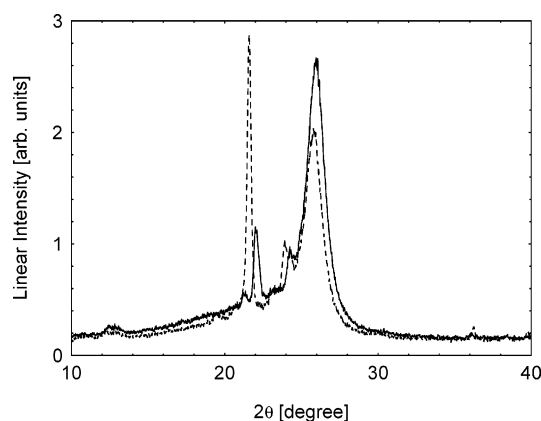


**Figure 11.** Wide-angle X-ray scattering curves of C36 powder crystallized from melt (dotted line) and from 4 wt % decane solution (solid line).

of 1 °C/min (not shown in Figure 10). As discussed above, the first (from the right) peak for pure C36 denotes crystallization to form a disordered rotator phase RIII, and the second peak shows a solid–solid phase transition from disordered rotator phase to ordered monoclinic structure.<sup>11,19,21</sup>

However, the crystals from 4% C36 in decane solution have only one broad peak. To test for the existence of the rotator phase in the crystals from solution, we quenched both pure C36 and 4% C36-in-decane samples from 80 °C to 0 °C in ca. two minutes. The crystals from solution were filtered and dried under vacuum at room temperature. Both were ground into powders and then observed by wide-angle X-ray scattering (WAXS). Figure 11 shows that the peak corresponding to the rotator structure appears in both samples, but the rotator peak for crystals from solution is small while that from melt is much higher, indicating that crystallization of C36 from decane solution suppresses the rotator phase. The faster diffusion and greater molecular mobility in solution favors the formation of the more stable monoclinic structure.

Another observation is that PEB affects the nucleation of C36 from solution. Figure 10 shows that PEB7.5 smoothes the onset and broadens the crystallization peak. PEB10 shows a stronger influence than PEB7.5. The crystallization temperature,  $T_{\text{cry}}$ , determined as the onset temperature of the appearance of the peak, is increased by about 1 °C and 1.5 °C for 4% C36 in decane by using 0.1 wt % PEB7.5 and 0.1 wt % PEB10, respectively.

Figure 12 depicts the effect of PEB10 and PEB7.5 on the morphology of C32 crystals from 4% decane solution. The morphology of the C32 crystals are decidedly more angular than the tapered C36 crystals; however the size of crystals decreases with increasing polymer concentration. For PEB7.5, the C32 crystals are larger than those of C36. In the case of PEB10, the yield stress can be reduced by almost 4 orders of magnitude at a polymer concentration as low as 500 ppm in decane.

A pure C32 melt shows two peaks at 67 and 62 °C in the DSC trace during cooling (Figure 13 top trace). The second peak is the rotator-to-monoclinic structure transition<sup>21</sup> also observed for C36 paraffin. The DSC curves for C36 and C32 in solution show one peak on cooling, suggesting that the rotator phase is absent or at low level. The influence of PEB10 and PEB7.5 on the DSC traces shows the same effect on 4%C32 as on 4%C36.

The morphology of C28 crystals from 4% decane

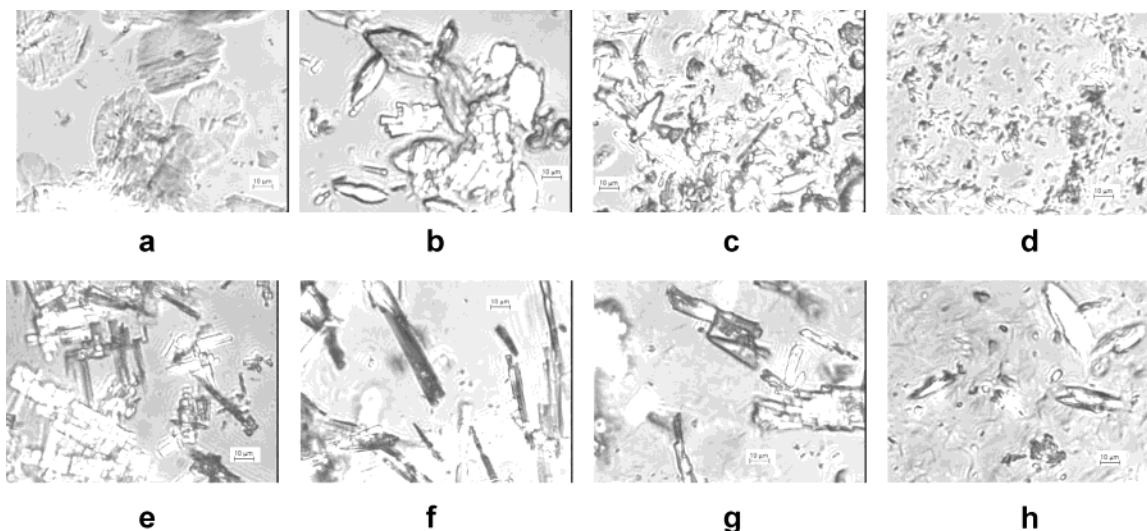


**Figure 12.** Optical micrographs of 4% C32 wax crystals under the effect of various amounts of PEB7.5 or PEB10 in decane at 0 °C. (a) 0.05 wt % PEB10; (b) 0.1 wt % PEB10; (c) 0.3 wt % PEB10; (d) 0.8 wt % PEB10; (e) 0.05 wt % PEB7.5; (f) 0.1 wt % PEB7.5; (g) 0.3 wt % PEB7.5; (h) 0.8 wt % PEB7.5.

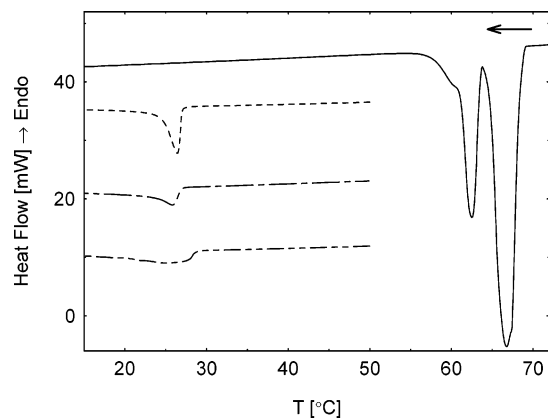


**Figure 13.** Comparison of DSC curves for different C32 samples. Curves from top to bottom are pure C32 (scan rate: 5 °C/min), 4% C32 in decane (scan rate: 5 °C/min), 4%C32 + 0.1%PEB7.5 (scan rate: 5 °C/min), and 4%C32 + 0.1%PEB10 (scan rate: 5 °C/min).

solution is different from that for C36 and C32 (Figure 14). The crystals form long sticks, especially when PEB7.5 is the modifier (Figure 14e, f, g). In the case of PEB10, the leaf-like crystal (Figure 14a) is also a raft consisting of densely connected sticks. When the concentration of PEB10 is over 0.1 wt %, the long sticks become small bars with significantly lower yield stresses. Since long aspect ratio sticks easily form network structures, all of the 4% C28 samples with PEB7.5 form gels with high yield stresses (Figure 8).

**3. PEB Effect on Paraffin Mixtures.** We now consider how the wax mixtures behave under the addition of PEB7.5 or PEB10. We begin with the mixture of 2%C36 + 2%C32 which showed cocrystallization. As expected, the crystals show shuttle-like or rod-like morphologies such as their mother paraffins (Figure 15). But the crystal size is much smaller than that of the pure 4%C36 and 4%C32. The relative yield stresses are higher than those of pure 4% C36 or 4%

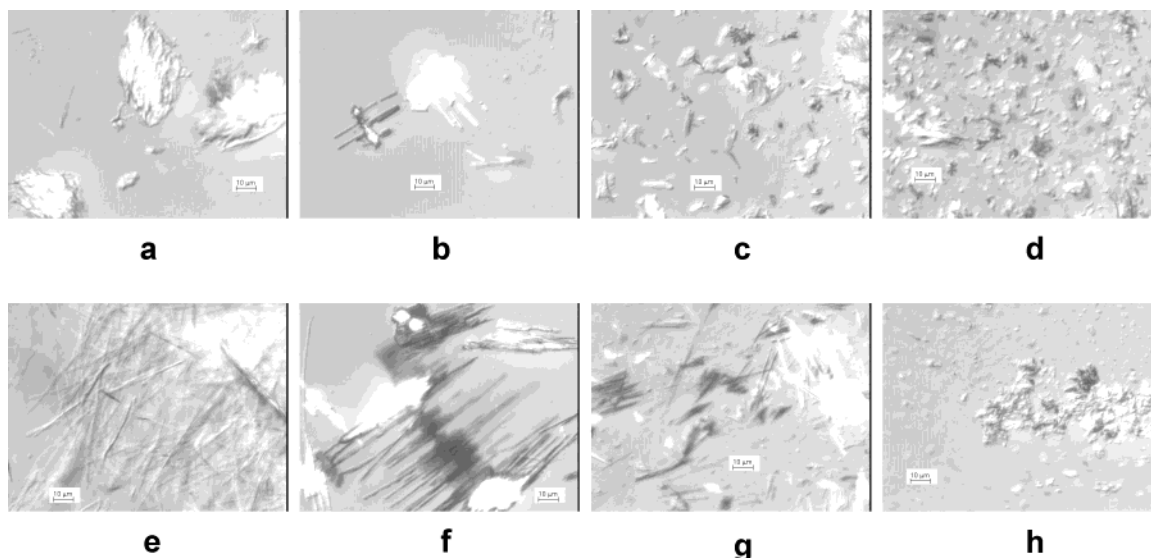


**Figure 14.** Optical micrographs of 4% C28 wax crystals under the effect of various amounts of PEB7.5 or PEB10 in decane at 0 °C. (a) 0.05 wt % PEB10; (b) 0.1 wt % PEB10; (c) 0.3 wt % PEB10; (d) 0.8 wt % PEB10; (e) 0.05 wt % PEB7.5; (f) 0.1 wt % PEB7.5; (g) 0.3 wt % PEB7.5; (h) 0.8 wt % PEB7.5.

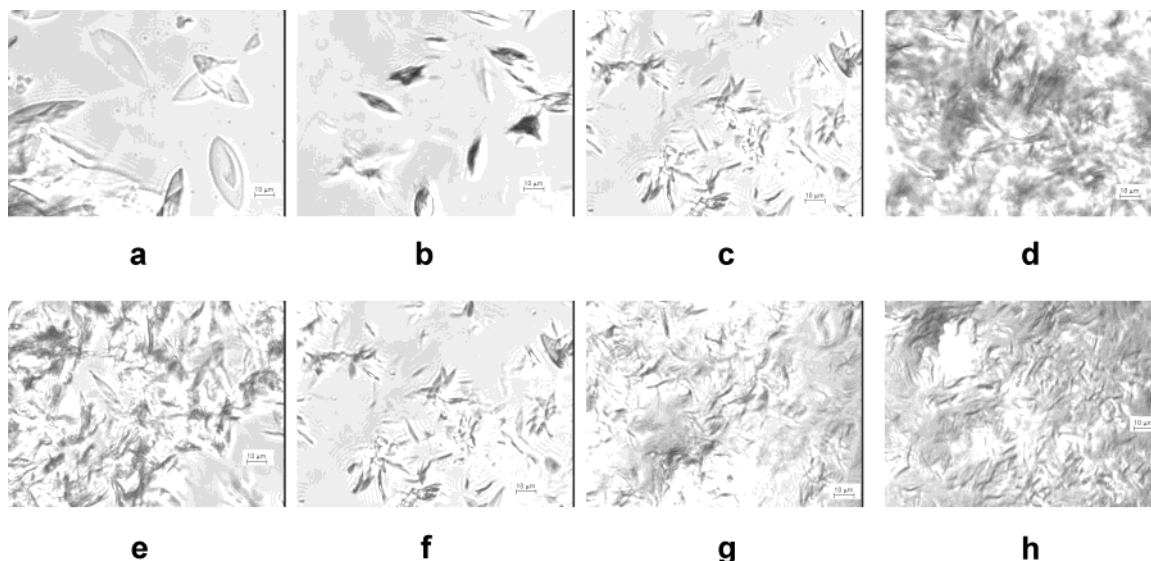


**Figure 15.** Optical micrographs of mixed wax 2%C36 + 2%C32 crystals under the effect of various amounts of PEB7.5 or PEB10 in decane at 0 °C. (a) 0.05 wt % PEB10; (b) 0.1 wt % PEB10; (c) 0.3 wt % PEB10; (d) 0.8 wt % PEB10; (e) 0.05 wt % PEB7.5; (f) 0.1 wt % PEB7.5; (g) 0.3 wt % PEB7.5; (h) 0.8 wt % PEB7.5.



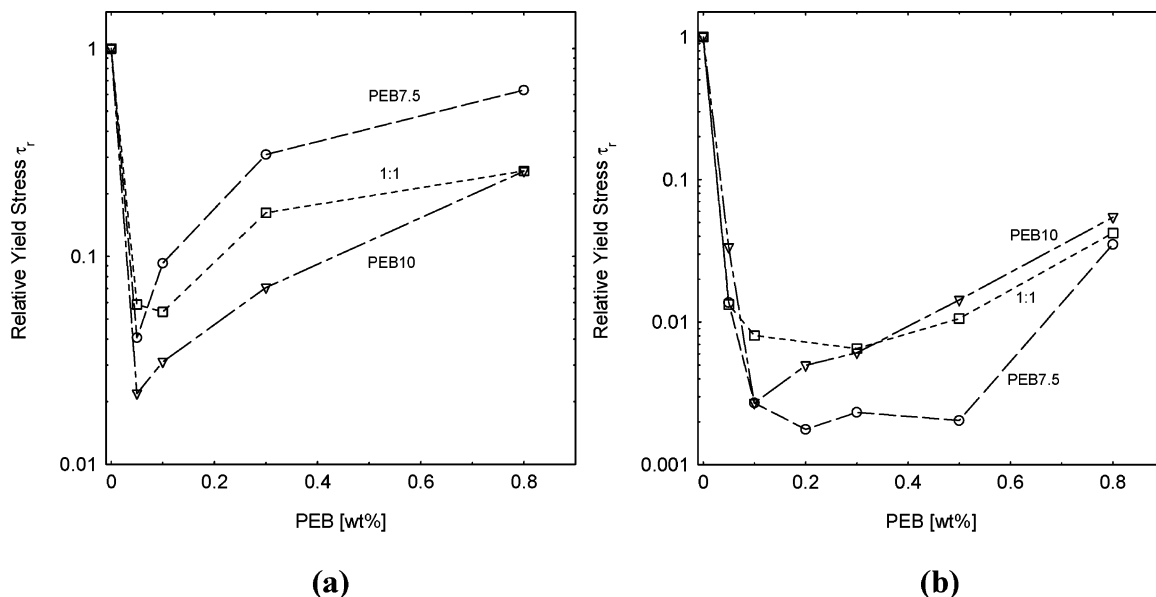


**Figure 16.** Effect of PEB7.5, PEB10 and their mixture on the relative yield stresses of wax mixtures. (a) 2%C36 + 2%C32: (○) PEB7.5; (□) 50 wt %PEB7.5 + 50 wt %PEB10; (▽) PEB10. (b) 2%C36 + 2%C28: (○) PEB7.5; (□) 50 wt %PEB7.5 + 50 wt %PEB10; (▽) PEB10.

C32: the polymers are less efficient at reducing the yield stresses of the mixed wax solutions than for the single-component wax solutions.

**4. Effect of Mixed PEB on Paraffin Mixtures.** In our previous study<sup>9</sup> we showed that the most efficient reduction in wax gel yield stress occurred when the paraffin carbon number was matched to the crystallizable ethyl runs on the PEB polymer. As a consequence, a single polymer can no longer be optimum for a mixture of paraffins. This motivates the question whether mixtures of PEBs can be chosen to minimize the yield stresses of a mixture of paraffins? But as shown in Figure 16, the mixture of PEB7.5 and PEB10 with equal weight amounts displays an intermediate effect from those of PEB 10 and PEB7.5 on decreasing the yield stresses of model waxy oils.

### Conclusion

The comparison of yield stresses of model waxy oils consisting of pure long chain paraffins and their binary mixtures in decane has shown that mixing the long chain paraffins reduces the yield stress significantly. DSC results revealed that the binary mixtures C36 + C32 and C32 + C28 show miscibility with only one crystallization peak, while C28 + C24, C36 + C28, C32 + C24, and C36 + C24 crystallize separately, as determined by the observation of two peaks upon cooling. Our observations agree with Kravchenko's

predictions<sup>21,28</sup> that the binary *n*-alkane mixtures in the case of  $\Delta n_c = 4$  have at least partial miscibility when the number of carbon atoms  $n_c$  is in the range of  $68 > n_c > 27$ , but crystallize separately when  $n_c < 28$ . Furthermore, we found that there is no miscibility when  $\Delta n_c > 4$ . The crystallization of paraffin from decane solution forms a stable crystal structure directly while from melt a disordered rotator phase occurs first, and then transforms to an ordered monoclinic structure on further cooling. Under the influence of PEB, the longer chain paraffins, such as C36, C32, or the mixtures containing them, crystallize into a uniform shape of rod-like (when the wax concentration is low) or shuttle-like (when the concentration of paraffin becomes higher) structure. However, C28 tends to form long sticks when modified by PEB. Both PEB7.5 and PEB10 are able to reduce significantly the yield stresses of model waxy oils consisting of single paraffins or their mixture. PEB10 seems more effective than PEB7.5 except for the mixture 2%C36 + 2%C28. The mix of PEBs leads to an average result which shows intermediate properties between those of single component.

**Acknowledgment.** We gratefully acknowledge support from the Halliburton Company and technical discussions with Dr. Lewis Norman and Dr. Ian D. Robb.

EF034098P